

An Effective Surface Design Based on a Graphene Oxide Decorated by Silver Nanoparticles for Detection of Carbofuran in Vegetable Samples

Dongshu Jia¹, Fengxian Qin¹, Bei Liu^{1,*}, Yujiao Tang¹, Yongjie Sun¹, Wei Chen^{1,*}

School of Life Sciences, Changchun Sci-Tech University, Changchun 130-600, China

*E-mail: cw15304477991@sina.com, jds18943969781@sina.com

Received: 8 February 2022 / Accepted: 29 March 2022 / Published: 7 May 2022

In this paper, a graphene oxide nanocomposite decorated with silver nanoparticles (Ag@GO) was used to modify a glass carbon electrode (GCE) as a nonenzymatic electrochemical sensor for detecting carbofuran (CF) in vegetable samples. According to surface morphology and crystal structure studies utilizing FESEM and XRD, the porous shape of the Ag@GO nanocomposite was generated by adorning the pure crystalline nature of the Ag NPs on the surface of GO sheets. DPV and amperometry were used to investigate the electrochemical properties of the Ag@GO/GCE, revealing that the modified electrode can be used as a comparable or better sensor for selective CF detection among the most commonly found compounds in real samples of fruits and vegetables than other reported CF sensors. According to the results, the modified electrode can detect CF in a wide detection range of 1 to 1000 μM , with a lower detection limit of 10 nM. Furthermore, the Ag@GO/GCE was employed to determine CF in real celery and lettuce samples and displayed efficient sensing ability, demonstrating that the Ag@GO/GCE has outstanding CF determination accuracy in vegetables.

Keywords: Nonenzymatic electrochemical sensor; Nanocomposite; Silver nanoparticles; Graphene oxide; Carbofuran; Vegetables

1. INTRODUCTION

Carbofuran (CF; 2,3-dihydro-2,2-dimethylbenzofuran-7-ol methyl carbamate), also known as furadan or curaterr, is a carbamate ester and a member of the 1-benzofuran family that is widely used in agriculture and forestry as a broad-spectrum systemic insecticide to control insects and worms [1-3]. The CF's low persistence and broad biological activity are crucial factors in its replacement of organochlorine insecticides that linger in the environment for a long time [4-6].

N-methyl carbamate, which is produced from carbamic acid and causes carbamylation of acetylcholinesterase at neural synapses and neuromuscular junctions, is involved in the mechanism of

action of CF [7, 8]. Thus, through the oral and inhalation routes of exposure, CF can affect the nervous system and cause weakness, breathing difficulties, sweating, cephalalgia, nausea, perspiration, vomiting, abdominal pain, dizziness, and blurred vision in humans, causing weakness, breathing difficulties, sweating, cephalalgia, nausea, perspiration, vomiting, abdominal pain, dizziness, and blurred vision [9, 10]. Higher levels can cause hypothermia, body tremors, muscular twitching, ascitations, loss of coordination, convulsions, and halted breathing, which can lead to death from respiratory failure [11, 12].

As a result, adequate, innovative, and effective approaches are required for determining and treating CF-contaminated fruits, vegetables, and wastewater [13, 14]. Many studies have been conducted to determine the CF level in CF-contaminated fruits, vegetables, and wastewaters through enzyme-linked immunosorbent assay (ELISA) [15], high-performance liquid chromatography [16], fluorimetry [17], gas chromatography [18], mass spectrometry [19], spectrophotometry [20], and electrochemical methods [21-26]. Between these approaches, electrochemical methods are quick, low-cost, and sensitive. Furthermore, in electrochemical approaches, the ability to promote and modify the electrode surface can improve the efficiency and selectivity of CF sensors. However, finding the right composition to increase the sensor's detection limit and liner range is crucial for use in fruit, vegetables, and wastewater samples. As a result, our research focused on the synthesis of Ag@GO nanocomposite modified GCE for CF detection in vegetable samples.

2. EXPERIMENTAL

2.1. Preparation of modified electrode

Prior to modification, the GCE was polished for 15 minutes on a micro-cloth pad with alumina powders (1.0 and 0.3 m, Hebei Suoyi New Material Technology Co., Ltd., China), then rinsed thoroughly with deionized water and ethanol, respectively, and dried in the air at room temperature. The Ag@GO nanocomposite was made in the following way [27], 160 ml NH_4 (40 wt%, Sigma-Aldrich) was gradually mixed with 20 ml of 0.02 M AgNO_3 ($\geq 99.0\%$, Sigma-Aldrich) solution using magnetic stirring, the stirring was continued to reach obvious solution, demonstrating to formation of silver ammonia complex $[\text{Ag}(\text{NH}_3)_2\text{OH}]$ [28]. Following that, 1 gram of GO (99.0%, Luoyang Tongrun Info Technology Co., Ltd., China) was ultrasonically added to the solution. For the reaction to proceed, the resulting suspension was microwave irradiated at 100 W for 120 seconds. After the reaction was completed, the mix was centrifuged for 5 minutes at 2000 rpm. The precipitate was cleaned multiple times with deionized water. 5 mL of Ag@GO nanocomposite was sprayed onto the GCE surface, air-dried, and used for electrochemical experiments right away.

2.2. Real sample preparation

The celery and lettuces were sliced into little pieces and provided by a local store. 10g of each sample was homogenized in a stainless steel blender before being ultrasonicated for 1 hour. The samples were then centrifuged for 10 minutes at 1000 rpm. The supernatants were then collected and

sprayed with a 2M CF concentration before being diluted to 10 mL in 0.1 M PBS (pH 7.4). For determination recovery and RSD values, the conventional addition approach was used.

2.3. Characterization of morphology, crystal structure and electrochemical properties

Field emission scanning electron microscopy (FESEM; JEOL, JSM-6700F, Japan) was used to examine the surface morphology of GO and Ag@GO nanocomposite. X-ray diffractometer (XRD; Bruker D8 DISCOVER, AXS GmbH, Karlsruhe, Germany) studies were used to investigate the crystallinity of GO and Ag@GO nanocomposite. DPV and amperometry techniques were used to investigate the electrochemical properties of Ag@GO/GCE in a conventional electrochemical cell that consisted of Ag@GO/GCE as the working electrode, platinum plate as the counter, and Ag/AgCl as the reference electrode, using a potentiostat-galvanostat (PGSTAT model 204 equipped with a module FRA32 M, Metrohm Autolab, Utrecht, The Netherlands). For DPV and amperometry measurements, a 0.1 M phosphate buffer solution (PBS, Sigma-Aldrich) with pH 7.4 was employed as the electrolyte.

3. RESULTS AND DISCUSSION

3.1. Studies of surface morphology and crystal structure

Figures 1a and 1b exhibit FESEM images of GO and Ag@GO nanocomposite modified GCE surface morphology. As observed in the SEM image of GO, there are smooth and thin sheet-like structures in a wave-like surface morphology that contain house-of-cards-type porous stacking structures. Because of the decoration of Ag NPs on the surface of GO sheets, the resultant porous morphology of the Ag@GO nanocomposite differs greatly from that of GO. As can be seen, a considerable number of Ag NPs in spherical shape are uniformly dispersed across the GO sheets. This porous shape can increase the electrode's effective surface area and analyte absorption capabilities [29, 30]. Studies have also shown that Ag NPs can interact with the GO sheets through physisorption, electrostatic binding, or charge-transfer interactions [31, 32]. The average diameter of Ag NPs is 55 nm.

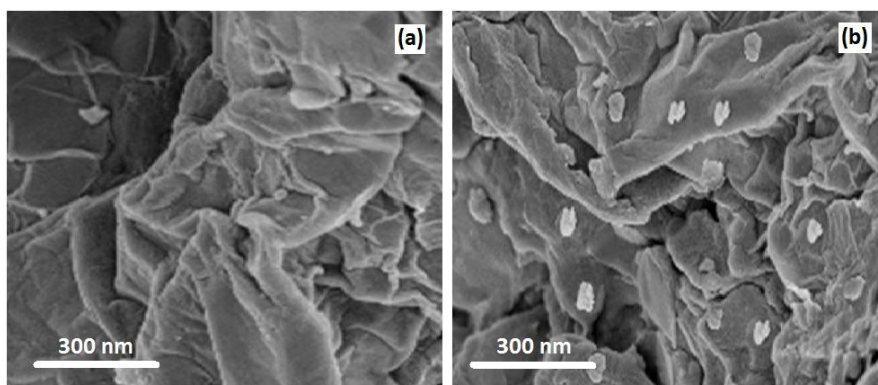


Figure 1. FESEM images of surface morphology (a) GO and (b) Ag@GO nanocomposite modified GCE.

Figure 2 shows the results of XRD examinations of GO and Ag@GO nanocomposite powders. The XRD pattern of GO reveals a distinct diffraction peak at 9.48° , which is attributed to the diffraction plane of GO (001) [33]. Additional diffraction peaks can be seen in the XRD pattern of Ag@GO nanocomposite at 38.18° , 44.06° , 64.34° , and 77.09° , which correspond to the development of face-centered cubic crystal phase of the metallic Ag with (111), (200), (220), and (311) reflections, respectively (JCPDS card no. 89-3722). The findings of the FESEM and XRD investigations show that the Ag NPs in the Ag@GO nanocomposite coated the GO sheets in a pure crystalline state.

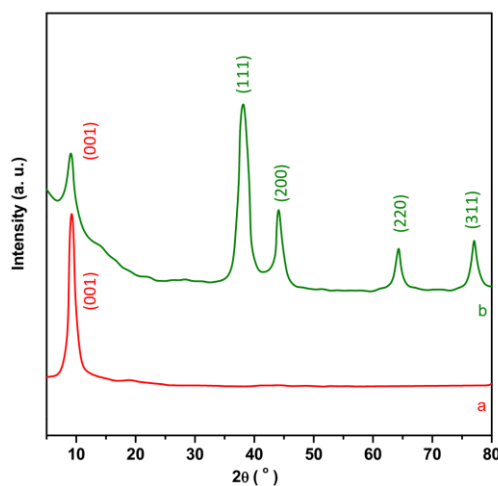


Figure 2. Result of XRD analyses of powders of (a) GO and (b) Ag@GO nanocomposite

3.2. Electrochemical Studies

Figure 3 presents the findings of GCE, GO/GCE, and Ag@GO/GCE DPV measurements in 0.1 M PBS (pH 7.4) in the absence and presence of $1\ \mu\text{M}$ CF at a scan rate of 20 mV/s. Both GCE and GO/GCE show no peak in the absence of $1\ \mu\text{M}$ CF, but Ag@GO/GCE shows an oxidation peak at 0.41 V, which is related to the oxidation of Ag^0 to Ag^+ ions [34, 35]. In the presence of $1\ \mu\text{M}$ CF, the DPV curves of GCE, GO/GCE and Ag@GO/GCE illustrate an oxidation peak at 0.20 V, 0.17 V and 0.10 V, respectively. It suggests that the CF oxidation mechanism involves hydrolysis of CF to carbofuran phenol an electrochemical active compound, and that the electrochemical oxidation of carbofuran phenol to a phenolic derivative of CF [36-38]. Comparison between the oxidation peak current of electrodes reveals that GO/GCE has lower potential and higher sensitivity to oxidation CF than that GCE because of the higher specific surface area of GO nanosheets, higher porosity and electrical conductivity of GO modified GCE [39, 40]. Furthermore, GO has several oxygen functional groups, including hydroxide and epoxide groups on the basal plane and carbonyl and carboxyl groups on the margins, which cause GO to behave as polar molecule adsorption sites [41, 42]. Moreover, compared to GO/GCE, Ag@GO/GCE has a lower potential and a higher sensitivity to oxidizing CF, showing that decorating Ag NPs on GO nanosheets increases electrode responsiveness. Ag NPs, which give additional charge carriers and ion transport channel ways, are thought to improve electrical

conductivity and porosity [43, 44], and the resulted nanocomposite could possess a greatly expanded and tuneable layered structure that provides channels for ions migration in electrochemical reactions [43, 45]. As a result, the Ag@GO nanocomposite's porous shape, conductivity, and polarity can enhance electrochemical response while lowering oxidation potential.

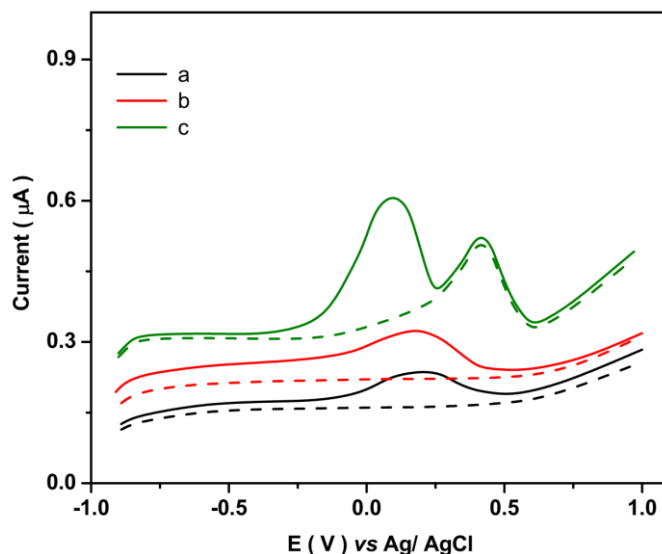


Figure 3. Results of DPV measurements of (a) GCE, (b) GO/GCE and (c) Ag@GO/GCE in 0.1 M PBS (pH 7.4) in absence (dashed lines) and presence (solid lines) of 1 μM CF at scan rate of 20 mV/s.

Figure 4 displays the amperometric response and calibration plot of Ag@GO/GCE during the successive addition of CF at regular intervals of 30 s into 0.1 M PBS (pH 7.4) at a potential of 0.10 V. As observed, with each addition of CF, the Ag@GO/GCE response is fast, and the amperometric current signal increases linearly while CF concentration increases in the range of 1 to 1000 μM with a correlation coefficient of 0.99925. The linear relationship is obtained as [46]:

$$I (\mu\text{A}) = 0.28949 [\text{CF}] (\mu\text{M}) + 0.06111 \quad (1)$$

The sensitivity and limit of detection (LOD) values are calculated to be 10 nM and 0.28949 $\mu\text{A}/\mu\text{M}$, respectively. Table 1 shows the sensing performance obtained from this investigation and other reported work in the literature. The Ag@GO/GCE performance is comparable to or better than that of other previously reported CF sensors, which can be related to the high electron transfer rate and robust electrocatalytic activity of the basal and edge structural defects on GO sheets [47]. It indicates that the incorporation of high conductive Ag NPs between GO sheets promotes the electrochemical signal. Ag NPs provide a bridge effect between the GO and GCE surface and improve the charge transfer rate [48, 49].

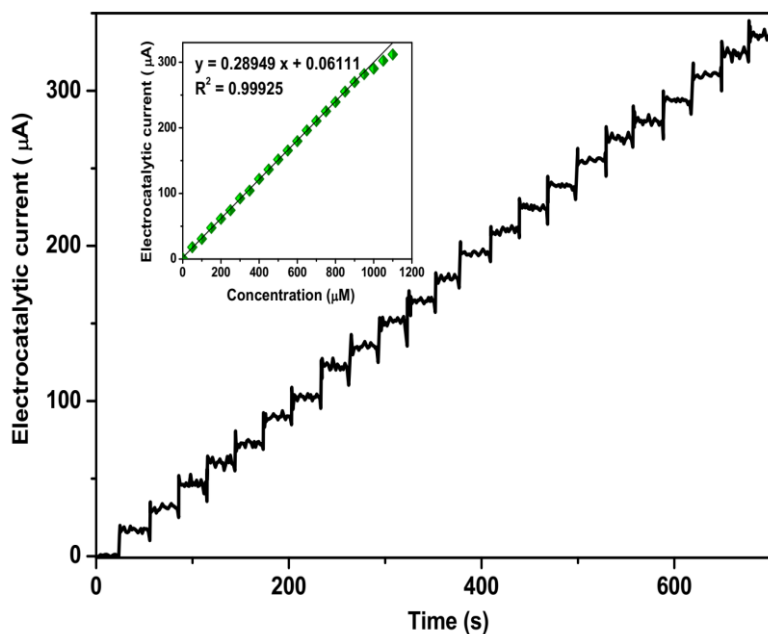


Figure 4. Amperometric and calibration plot of Ag@GO/GCE during the successive addition of CF at regular intervals of 30 s into 0.1 M PBS (pH 7.4) at potential of 0.10 V.

Table 1. The obtained sensing performance of this study and the other reported work in the literature.

Electrode	Technique	LOD (nM)	Linear range (µM)	Ref.
Ag@GO/GCE	AMP	10	1–1000	This work
Anti-carbofuran monoclonal antibody/silica sol-gel/GCE	CV	1.5	226–904	[23]
Au NPs@ RGO /GCE	DPV	20	0.05–20	[21]
Gadolinium sulfide/RGO/ GCE	CV	12.8	10 ⁻³ –1381	[22]
CoO decorated RGO	DPV	19	0.5–200	[24]
Ni NPs/ionic liquid /GCE	CV	500	5.0–305	[50]
Heated screen-printed carbon electrode	DPV	50	0.4–400	[51]
Isolated endophytic fungus Eupenicillium shearii FREI-39 esterase/ MWCNTs/ halloysite,	SWV	7.6	0.022–0.452	[52]
Acetylcholinesterase/Fe ₃ O ₄ - chitosan /GCE	SWV	3.6	0.005–0.09	[53]
Hemin and nickel (II)/octabutoxy-29H, 31H-phthalocyanine complex /carbon paste electrode	FIA	1700	50–1000	[54]
Poly(3,4-ethylenedioxythiophene)/polystyrene sulphoanate/GO	LSV	100	1–90	[55]

AMP: Amperometry; SWV: Square wave voltammetry; FIA: Flow-Injection Analysis; LSV: Linear sweep voltammetry

Table 2 shows the results of interference studies of Ag@GO/GCE to determine CF using amperometric analysis in 0.1 M PBS (pH 7.4) at a potential of 0.10 V. These measurements included

investigation of the amperometric response of the proposed electrode to determination of CF and a 5-fold of the most commonly found compounds in real samples of fruits and vegetables [24, 56, 57]. Findings illustrates that the sensor's response to CF is significantly more than that interfering substances, and the negligible response is observed to additional interference compounds, indicating that the substances presented in Table 2 do not interfere with CF determination. Thus, the present sensor could be used for the rapid and selective detection of CF.

Table 2. Results of study the interfering effect of most commonly found compounds in real samples of fruits and vegetables on the amperometric determination of CF using Ag@GO/GCE at potential of 0.10 V under in 0.1 M PBS (pH 7.4).

Substance	Added (μM)	Amperometric signal (μA)	RSD (%)
CF	1.00	0.29	± 0.0373
Ascorbic acid	5.00	0.03	± 0.0081
Leucine	5.00	0.04	± 0.0021
3-hydroxycarbofuran	5.00	0.04	± 0.0018
Xanthine	5.00	0.05	± 0.0029
Hydroquinone	5.00	0.01	± 0.0014
Tartrate	5.00	0.02	± 0.0013
Glucose	5.00	0.01	± 0.0015
Guanine	5.00	0.03	± 0.0008
Catechol	5.00	0.01	± 0.0019
Caffeine	5.00	0.03	± 0.0112
Glycine	5.00	0.05	± 0.0038
Bicarbonate	5.00	0.02	± 0.0045
Carbaryl	5.00	0.07	± 0.0037
Tartrate	5.00	0.02	± 0.0011
Methiocarb	5.00	0.02	± 0.0016
Ca^{2+}	5.00	0.02	± 0.0027
Cu^{2+}	5.00	0.03	± 0.0029
K^+	5.00	0.02	± 0.0070
Na^+	5.00	0.01	± 0.0037
SO_4^{2-}	5.00	0.03	± 0.0011
Mg^{2+}	5.00	0.02	± 0.0013
Al^{3+}	5.00	0.03	± 0.0022
Zn^{2+}	5.00	0.01	± 0.0019
CO_3^{2-}	5.00	0.02	± 0.0033
NO^-	5.00	0.03	± 0.0073
SO_3^{2-}	5.00	0.02	± 0.0009
F^-	5.00	0.04	± 0.0011
Cl^-	5.00	0.07	± 0.0055

3.3. Analysis of real samples

Using an amperometric approach at a potential of 0.10 V in prepared 0.1 M PBS (pH 7.4) and real samples of celeries and lettuces, the practical capacity of Ag@GO/GCE to detect CF in prepared genuine samples of celeries and lettuces was assessed. Figures 6a and 6b illustrate amperometric measurements and corresponding calibration plots of genuine samples of celeries and lettuces in prepared 0.1 M PBS with progressive additions of CF solutions, respectively. The CF concentration in prepared 0.1 M PBS with genuine samples of celery and lettuce is 1.03 μM and 1.02 μM , respectively, as seen in the calibration graphs in Figures 6a and 6b, meaning that the CF content in pure real samples of celeries and lettuces is 2.06 μM and 2.04 μM , respectively. These concentrations are quite close to the first CF solution concentration sprayed on samples during the preparation process. As a result, the CF levels in the celery and lettuce samples were assessed to be 0.06 μM and 0.04 μM , respectively. The obtained recovery (95.66% to 97.60% for celeries and 93.00% to 99.00% for lettuce samples) and RSD (3.21% to 4.44% for celeries and 2.33% to 4.19% for lettuce samples) indicate that the Ag@GO/GCE has excellent CF determination accuracy in vegetables, as shown in Table 3.

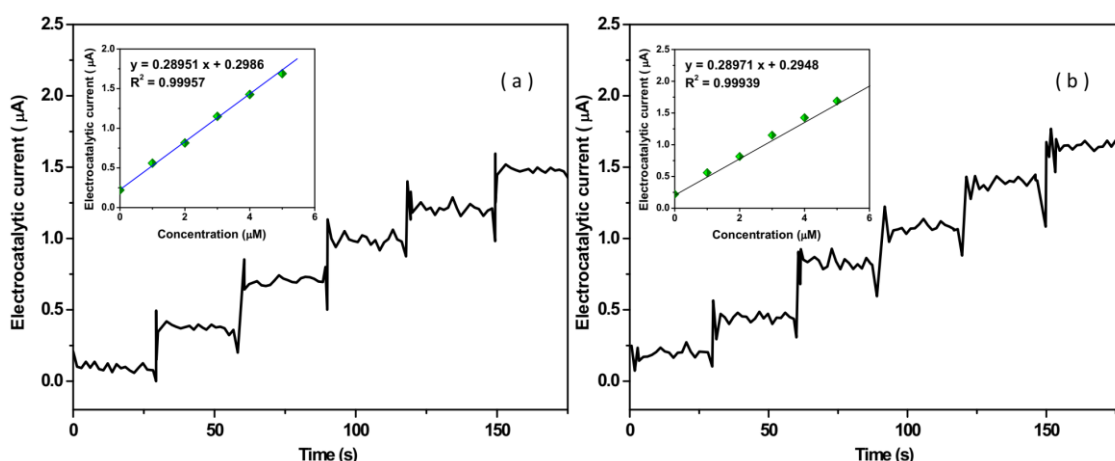


Figure 6. Amperometric measurements and related calibration plots of Ag@GO/GCE to addition of CF solution at potential of 0.10 V in prepared 0.1 M PBS (pH 7.4) with real samples of (a) celeries and (b) lettuces.

Table 3. Analytical findings of determination of CF in the celeries and lettuces samples

Sample	added(μM)	Found(μM)	Recovery(%)	RSD(%)
Celery	1.00	0.96	96.00	3.21
	2.00	1.95	97.50	2.39
	3.00	2.87	95.66	4.22
	4.00	3.90	97.50	4.44
	5.00	4.88	97.60	3.87
Lettuce	1.00	0.93	93.00	2.33
	2.00	1.90	95.00	2.79
	3.00	2.97	99.00	3.41
	4.00	3.89	97.25	4.19
	5.00	4.92	98.40	3.79

4. CONCLUSION

The measurement of CF in vegetable samples was proposed in this work using an effective surface design based on Ag@GO/GCE as an electrochemical sensor. According to the results of surface morphology and crystal structure research, the porous morphology of the Ag@GO nanocomposite was generated on the GCE surface by adorning the pure crystalline nature of Ag NPs on the surface of GO sheets. According to electrochemical experiments, the proposed electrode can be employed as a comparable or better sensor than existing reported CF sensors for selective CF detection among the most frequently observed chemicals in real samples of fruits and vegetables. The modified electrode can detect CF in a wide detection range of 1 to 1000 μM , with a lower detection limit of 10 nM, according to the results. Furthermore, the Ag@GO/GCE was used to determine CF in real samples of celery and lettuce, and it demonstrated efficient sensing ability. The RSD (3.21 to 4.44 percent for celeries and 2.33 to 4.19 percent for lettuce samples) and recovery (95.66 to 97.60 percent for celeries and 93.00 to 99.00 percent for lettuce samples) values obtained using the standard addition technique demonstrated that the Ag@GO/GCE has excellent accuracy for CF determination in vegetables.

References

1. X. Tang, J. Wu, W. Wu, Z. Zhang, W. Zhang, Q. Zhang, W. Zhang, X. Chen and P. Li, *Analytical chemistry*, 92 (2020) 3563.
2. W. Liu, Y. Zheng, Z. Wang, Z. Wang, J. Yang, M. Chen, M. Qi, S. Ur Rehman, P.P. Shum and L. Zhu, *Advanced Materials Interfaces*, 8 (2021) 2001978.
3. X. Wu, C. Li, Z. Zhou, X. Nie, Y. Chen, Y. Zhang, H. Cao, B. Liu, N. Zhang and Z. Said, *The International Journal of Advanced Manufacturing Technology*, 117 (2021) 2565.
4. R. Dobšíková, *Plant Protection Science*, 39 (2003) 103.
5. H. Zhu, J. Zhu, Z. Zhang and R. Zhao, *The Journal of Physical Chemistry C*, 125 (2021) 26542.
6. T. Gao, C. Li, Y. Wang, X. Liu, Q. An, H.N. Li, Y. Zhang, H. Cao, B. Liu and D. Wang, *Composite Structures*, 286 (2022) 115232.
7. R.C. Gupta, *Journal of Toxicology and Environmental Health, Part A Current Issues*, 43 (1994) 383.
8. T. Ishigami, K. Amano, A. Fujii, Y. Ohmukai, E. Kamio, T. Maruyama and H. Matsuyama, *Separation and purification technology*, 99 (2012) 1.
9. Z. Zhang, Y. Lou, C. Guo, Q. Jia, Y. Song, J.-Y. Tian, S. Zhang, M. Wang, L. He and M. Du, *Trends in Food Science & Technology*, 118 (2021) 569.
10. N.I.M. Ruzaidy and A. Amid, *Science Heritage Journal (GWS)*, 4 (2020) 1.
11. J.K. Gupta and S. Gupta, *Acta Informatica Malaysia*, 3 (2019) 4.
12. H. Li, Y. Zhang, C. Li, Z. Zhou, X. Nie, Y. Chen, H. Cao, B. Liu, N. Zhang and Z. Said, *The International Journal of Advanced Manufacturing Technology*, (2022) 1.
13. M. Nazeer, F. Hussain, M.I. Khan, E.R. El-Zahar, Y.-M. Chu and M. Malik, *Applied Mathematics and Computation*, 420 (2022) 126868.
14. H. Karimi-Maleh, C. Karaman, O. Karaman, F. Karimi, Y. Vasseghian, L. Fu, M. Baghayeri, J. Rouhi, P. Senthil Kumar and P.-L. Show, *Journal of Nanostructure in Chemistry*, (2022) 1.
15. J. Yang, H. Wang, Y. Jiang, Y. Sun, K. Pan, H. Lei, Q. Wu, Y. Shen, Z. Xiao and Z. Xu, *Molecules*, 13 (2008) 871.

16. A. Abad, M.a.J. Moreno, R. Pelegrí, M.a.I. Martínez, A. Sáez, M. Gamón and A. Montoya, *Journal of Chromatography A*, 833 (1999) 3.
17. N.L. Pacioni and A.V. Veglia, *Analytica Chimica Acta*, 488 (2003) 193.
18. B.C. Leppert, J.C. Markle, R.C. Helt and G.H. Fujie, *Journal of agricultural and food chemistry*, 31 (1983) 220.
19. A. Detomaso, G. Mascolo and A. Lopez, *Rapid Communications in Mass Spectrometry: An International Journal Devoted to the Rapid Dissemination of Up-to-the-Minute Research in Mass Spectrometry*, 19 (2005) 2193.
20. J.R. Rangaswamy, Y.N. VijayaShankar and S.R. Prakash, *Journal of the Association of Official Analytical Chemists*, 59 (1976) 1276.
21. X. Tan, Q. Hu, J. Wu, X. Li, P. Li, H. Yu, X. Li and F. Lei, *Sensors and Actuators B: Chemical*, 220 (2015) 216.
22. V. Mariyappan, M. Keerthi and S.-M. Chen, *Journal of Agricultural and Food Chemistry*, 69 (2021) 2679.
23. X. Sun, S. Du, X. Wang, W. Zhao and Q. Li, *Sensors*, 11 (2011) 9520.
24. M. Wang, J. Huang, M. Wang, D. Zhang and J. Chen, *Food chemistry*, 151 (2014) 191.
25. Y. Yang, Y. Zhou, Y. Liang and R. Wu, *International Journal of Electrochemical Science*, 16 (2021) 210616.
26. M. Pohanka, J. Fusek, V. Adam and R. Kizek, *International Journal of Electrochemical Science*, 8 (2013) 71.
27. P. Rameshkumar, N. Yusoff, H.N. Ming and M.S. Sajab, *Ceramics International*, 42 (2016) 18813.
28. A.M. Golsheikh, N. Huang, H. Lim and R. Zakaria, *Rsc Advances*, 4 (2014) 36401.
29. L. Ge, S. Wang, J. Yu, N. Li, S. Ge and M. Yan, *Advanced Functional Materials*, 23 (2013) 3115.
30. N.M. Mohamed, R. Bashiri, F.K. Chong, S. Sufian and S. Kakooei, *international journal of hydrogen energy*, 40 (2015) 14031.
31. S. Khorrami, Z. Abdollahi, G. Eshaghi, A. Khosravi, E. Bidram and A. Zarrabi, *Scientific Reports*, 9 (2019) 9167.
32. H. Maleh, M. Alizadeh, F. Karimi, M. Baghayeri, L. Fu, J. Rouhi, C. Karaman, O. Karaman and R. Boukherroub, *Chemosphere*, (2021) 132928.
33. A.R. Ridzuan, S. Ibrahim, S. Karman, M.S. Ab Karim, W.S.W.K. Zaman and C.C. Khuen, *International Journal of Electrochemical Science*, 16 (2021) 210557.
34. M.M. Abudabbus, I. Jevremović, K. Nešović, A. Perić-Grujić, K.Y. Rhee and V. Mišković-Stanković, *Composites Part B: Engineering*, 140 (2018) 99.
35. T.H. Zhao, M.I. Khan and Y.M. Chu, *Mathematical Methods in the Applied Sciences*, (2021) 1.
36. C.M. Miyazaki, A.M. Adriano, R.J. Rubira, C.J. Constantino and M. Ferreira, *Journal of Environmental Chemical Engineering*, 8 (2020) 104294.
37. A.N. Solomonenko, E.V. Dorozhko, J. Barek, E.I. Korotkova, V. Vyskocil and A.V. Shabalina, *Journal of Electroanalytical Chemistry*, 900 (2021) 115692.
38. N. Naderi, M. Hashim, J. Rouhi and H. Mahmodi, *Materials science in semiconductor processing*, 16 (2013) 542.
39. J. Li, J. Liu, G. Tan, J. Jiang, S. Peng, M. Deng, D. Qian, Y. Feng and Y. Liu, *Biosensors and Bioelectronics*, 54 (2014) 468.
40. H. Li, Y. Zhang, C. Li, Z. Zhou, X. Nie, Y. Chen, H. Cao, B. Liu, N. Zhang and Z. Said, *Korean Journal of Chemical Engineering*, (2022) 1.
41. S. Alipoori, M. Torkzadeh, M.M. Moghadam, S. Mazinani, S.H. Aboutalebi and F. Sharif, *Polymer*, 184 (2019) 121908.
42. Y.-M. Chu, U. Nazir, M. Sohail, M.M. Selim and J.-R. Lee, *Fractal and Fractional*, 5 (2021) 119.

43. I.-H. Cho, D.H. Kim and S. Park, *Biomaterials research*, 24 (2020) 1.
44. H. Karimi-Maleh, R. Darabi, M. Shabani-Nooshabadi, M. Baghayeri, F. Karimi, J. Rouhi, M. Alizadeh, O. Karaman, Y. Vasseghian and C. Karaman, *Food and Chemical Toxicology*, 162 (2022) 112907.
45. J. Park, J. Lee, S. Kim and J. Hwang, *Materials*, 14 (2021) 2597.
46. Y.-M. Chu, B. Shankaralingappa, B. Gireesha, F. Alzahrani, M.I. Khan and S.U. Khan, *Applied Mathematics and Computation*, 419 (2022) 126883.
47. P.K. Kannan, S.A. Moshkalev and C.S. Rout, *Nanotechnology*, 27 (2016) 075504.
48. K.-S. Kim and S.-J. Park, *Synthetic metals*, 162 (2012) 2107.
49. Z. Said, S. Arora, S. Farooq, L.S. Sundar, C. Li and A. Allouhi, *Solar Energy Materials and Solar Cells*, 236 (2022) 111504.
50. H. Baksh, J.A. Buledi, N.H. Khand, A.R. Solangi, A. Mallah, S.T. Sherazi and M.I. Abro, *Monatshefte Für Chemie-Chemical Monthly*, 151 (2020) 1689.
51. H. Wei, J.-J. Sun, Y.-M. Wang, X. Li and G.-N. Chen, *Analyst*, 133 (2008) 1619.
52. G.F. Grawe, T.R. de Oliveira, E. de Andrade Narciso, S.K. Moccelini, A.J. Terezo, M.A. Soares and M. Castilho, *Biosensors and Bioelectronics*, 63 (2015) 407.
53. T. Jeyapragasam and R. Saraswathi, *Sensors and Actuators B: Chemical*, 191 (2014) 681.
54. A. Wong and M.D.P.T. Sotomayor, *Journal of Electroanalytical Chemistry*, 731 (2014) 163.
55. F. Chekol, S. Mehretie, F.A. Hailu, T. Tolcha, N. Megersa and S. Admassie, *Electroanalysis*, 31 (2019) 1104.
56. D.P. Nikolelis, G. Raftopoulou, N. Psaroudakis and G.P. Nikoleli, *Electroanalysis: An International Journal Devoted to Fundamental and Practical Aspects of Electroanalysis*, 20 (2008) 1574.
57. A. Ejaz, H. Babar, H.M. Ali, F. Jamil, M.M. Janjua, I.R. Fattah, Z. Said and C. Li, *Sustainable Energy Technologies and Assessments*, 46 (2021) 101199.